

## Structure of micelles at interfaces

This article has been downloaded from IOPscience. Please scroll down to see the full text article.

2005 J. Phys.: Condens. Matter 17 S3645

(<http://iopscience.iop.org/0953-8984/17/45/060>)

View [the table of contents for this issue](#), or go to the [journal homepage](#) for more

Download details:

IP Address: 129.252.86.83

The article was downloaded on 28/05/2010 at 06:44

Please note that [terms and conditions apply](#).

# Structure of micelles at interfaces

Max Wolff<sup>1,2</sup>, Andreas Magerl<sup>3</sup> and Hartmut Zabel<sup>2</sup>

<sup>1</sup> Institute Laue-Langevin, BP 156, 38000 Grenoble Cedex 9, France

<sup>2</sup> Lehrstuhl für Festkörperphysik, Universitätsstrasse 150, 44780 Bochum, Germany

<sup>3</sup> Lehrstuhl für Kristallographie und Strukturphysik, Staudtstrasse 3, 91058 Erlangen, Germany

E-mail: [v-wolff@ill.fr](mailto:v-wolff@ill.fr)

Received 15 September 2005

Published 28 October 2005

Online at [stacks.iop.org/JPhysCM/17/S3645](http://stacks.iop.org/JPhysCM/17/S3645)

## Abstract

In aqueous solutions and for high concentrations, tri-block copolymers are known to aggregate. As a critical volume fraction of micelles is reached, they crystallize. We have studied the temperature dependence of the structure formed by Pluronic P85 micelles solved in deuterated water close to an attractive and a repulsive wall. We find that the cubic structure is suppressed for the repulsive surface and for both interfaces during cooling.

(Some figures in this article are in colour only in the electronic version)

## 1. Introduction

The understanding of self-assembling at the molecular scale in the vicinity of a solid substrate is a key issue for the fabrication of nanodevices [1–3]. As the interaction between polymer micelles as well as the interaction between the micelles and a substrate can be varied continuously by changing the temperature, concentration or pressure, micellar systems offer a model system for the study of gelation or crystallization [4–11]. Recently we have demonstrated that by use of grazing incident small angle neutron scattering (GISANS) the structure close to solid interfaces becomes visible [12]. For a decreased internal micelle stability the influence of the interface was found less pronounced [13], and shear aligns a sample more in the bulk than close to the interface [14]. In the present study we characterize the influence of temperature on the crystallization of micelles from bulk solution close to solid interfaces. We find different structural phases for the same temperatures at interfaces with distinct chemical terminations and for the same interface for different sample histories.

## 2. Experimental details

The sample, Pluronic P85 (EO<sub>25</sub>–PO<sub>40</sub>–EO<sub>25</sub>), was obtained from BASF Wyandotte Corp. (New Jersey, USA) and used without further purification. The bulk properties of

this polymer are known in great detail [15]. Pluronics tend to self-assemble in aqueous solutions. The resulting aggregations have a hydrophobic core and hydrophilic shell and could be described as hard spheres with an attractive shell. At a critical micelle volume fraction, a percolation transition is observed [4–6]. For our experiment, P85 was diluted to 33% (in weight) in deuterated water and filled into the sample cell in the liquid phase.

Two single-crystalline polished silicon disks were prepared as solid interfaces. One was oxidized for 15 min in a 5:1 mixture of  $\text{H}_2\text{SO}_4$  and  $\text{H}_2\text{O}_2$  resulting in a hydrophilic (attractive)  $\text{SiO}_2$  termination (contact angle of water  $33^\circ$ ). The second substrate was cleaned with the same mixture of acids and a deposition by exposure to gaseous HDMS (1,1,1,3,3,3-hexamethyldisiazane) was made for 24 h to achieve a hydrophobic (repulsive) termination (contact angle of water  $75^\circ$ ) [16].

With GISANS, correlations perpendicular and parallel to an interface can be probed on the ångström length scale. Neutron reflectivity provides additional information in the micrometre range. A more detailed description of the technique can be found in [13]. A monochromatic neutron beam enters a silicon block from the side and becomes scattered at the solid–liquid interface. The intensity is then registered by a position-sensitive detector.

The measurements were carried out with the instruments ADAM and D22 at the Institute Laue-Langevin (Grenoble, France) using an incoming wavelength of  $\lambda = 4.41 \text{ \AA} \pm 1\%$  and  $6 \text{ \AA} \pm 10\%$ , respectively. On D22 a 8 m collimation was used. For the rocking scans with the ADAM instrument, the incident beam was collimated by two slits with an opening of 2 mm each and a separation of 2 m. For the GISANS measurement, two additional slits with a separation of 1 m collimated the beam in the direction perpendicular to the scattering plane.

The thickness of our samples was 1 mm. For low incoming angles ( $<1^\circ$ ), the penetration depth, parallel to the surface normal, of the neutron beam into the sample is of the order of 100  $\mu\text{m}$ . The normal of the interface was oriented horizontally for all measurements.

For the repulsive interface and the rocking curves for the attractive one, the heating and cooling rate was about  $0.1 \text{ }^\circ\text{C min}^{-1}$ . For the GISANS measurements at the attractive interface, the sample was heated in 1 h from 15 to  $60^\circ\text{C}$  and cooled down in 2 h.

### 3. Experimental results

Figure 1 shows the scattered intensity plotted on a logarithmic scale for different rocking angles and temperatures. The dashed line marks the angle at which the GISANS data were taken. The left panel depicts the result of the measurement with the sample in contact with the attractive interface. With increasing and decreasing temperature nine sections (1–5 and 1'–4') can be clearly distinguished and identified with the phases found earlier in a small-angle scattering study [17]. At low temperatures ( $T < 24^\circ\text{C}$ , phase 1) the sample is in a liquid micellar phase and no Bragg reflection is visible. Then by crossing the border to the cubic phase (phase 2) a very sharp and narrow peak shows up. With further increasing temperature this reflection seems to become diffusely broadened before it disappears at  $57^\circ\text{C}$ , when the sample melts to the rod-like micelle phase (phase 3). At  $59^\circ\text{C}$  again a narrow and intense reflection shows up and the micelles form a hexagonal structure (phase 4). At about  $80^\circ\text{C}$  the crystalline structure melts (phase 5). While cooling the sample we observe similar regions of increased intensity. The phases that should correspond to the heating are marked with the same but primed numbers.

The right panel in figure 2 shows the scattered intensity for the sample in contact with the repulsive interface. Again for low and high temperatures the Bragg reflection is missing and the crystalline structure melted. Instead of the rod-like micelle phase (3) in proximity to the attractive interface, we now find an increased intensity. In addition, in the crystalline phases

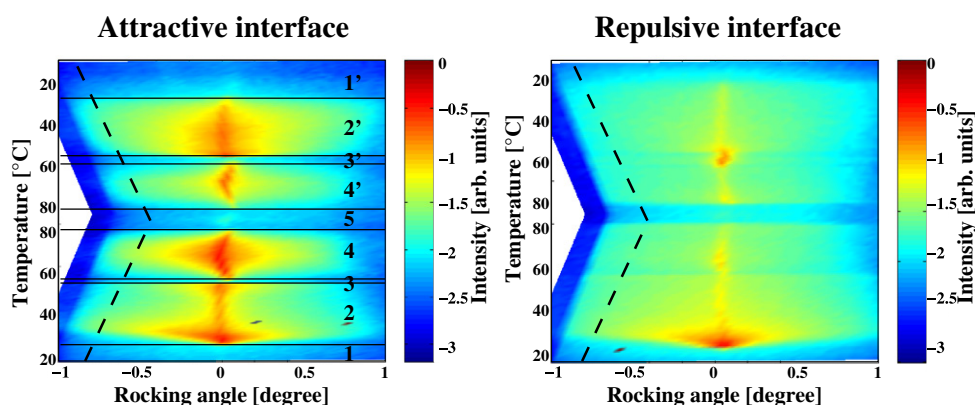


**Figure 1.** Intensity maps plotted for different rocking angles and temperatures either with the sample in contact with an attractive (left panel) or a repulsive interface (right panel).

(2, 4) the intensity is clearly decreased, except for the first crystallization into the cubic phase (1 into 2).

To draw a more detailed picture we have evaluated the  $Q_{\perp}$  value of the first-order Bragg reflection (see figure 2). The zero in the rocking curves shown in figure 1 was set to the centre of the reflection for the particular temperature. The peak position (figure 2 panel (a)) decreases linearly with temperature in the crystalline phases until a minimum value of  $0.0515 \text{ \AA}^{-1}$  is reached for both interfaces [17]. The transition from the cubic to the hexagonal phase is clearly visible from the sudden increase in  $Q_{\perp}$  for the attractive interface which is missing for the repulsive one, at which in addition the lattice parameter is found to be slightly smaller.

The integrated intensities from fits to the rocking curves are shown in figures 2(b)–(d). The rocking curves have been fitted with two components. The narrow one is resolution limited and represents long-range orientational correlations, and the wider one is broadened due to mosaicity or the crystallite size. The intensity of the narrow line is shown in figure 2 panel (b). For both interfaces a clear increase in the intensity is visible when the cubic phase (2) is reached from low temperatures. For the attractive interface for all temperatures in the cubic phase (2) a significant contribution of the narrow line is visible and disappears finally when the rod-like micelle phase (3) is reached. Within the hexagonal phase (4) we find the highest intensity in the centre of the phase. The intensity distribution for the attractive interface during cooling is qualitatively similar but less pronounced, again with a small peak when phase (3') is entered. For the repulsive interface we find a completely different behaviour. The intensity drops quickly after the cubic phase is formed and stays low except for the clear peak in the rod-like micelle phase.

For the intensity of the wider component (figure 2, panel (c)) we find qualitatively the same behaviour for both interfaces in the cubic phase (2) with an enhanced intensity when the phase is reached during heating the sample. For the attractive interface the intensity in addition clearly peaks in the centre of the hexagonal phase similar to the narrow component. During cooling, the intensity for phase 2' is only increased for the attractive interface. In the rod-like micelle phase again the intensity is higher for the repulsive interface.

Panel (d) (figure 2) depicts the correlation length parallel to the interface calculated from the line width of the broader component. It turns out that for both interfaces first correlations develop over large length scales when the cubic phase (2) is entered. For the attractive interface the correlation length is in addition large for temperatures close to the rod-like micelle phase

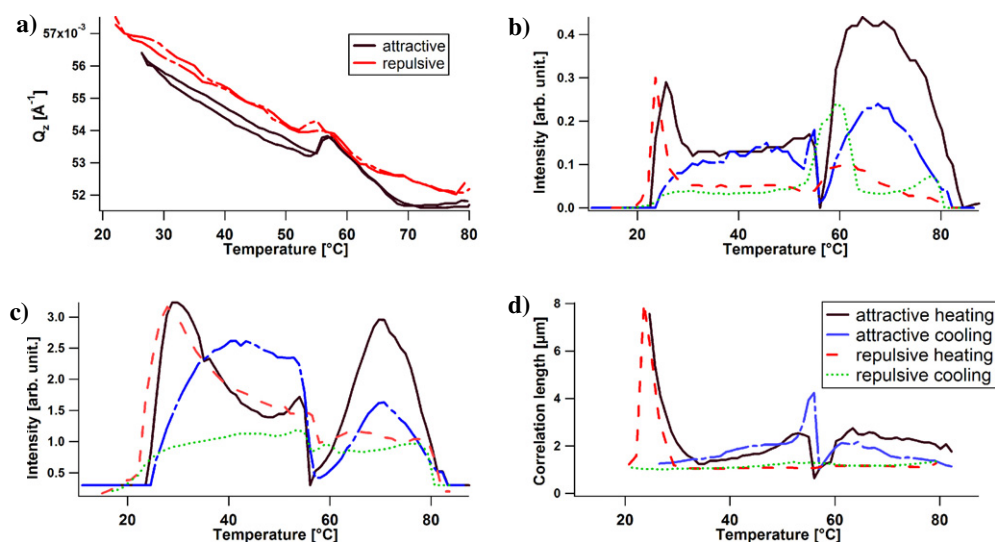


**Figure 2.**  $Q$ -value of the Bragg reflection (panel (a)), intensities (narrow line (panel (b)) and broad line (panel (c))) and correlation length (panel (d)) extracted from a fit with two lines to the data shown in figure 1 plotted for different temperatures.

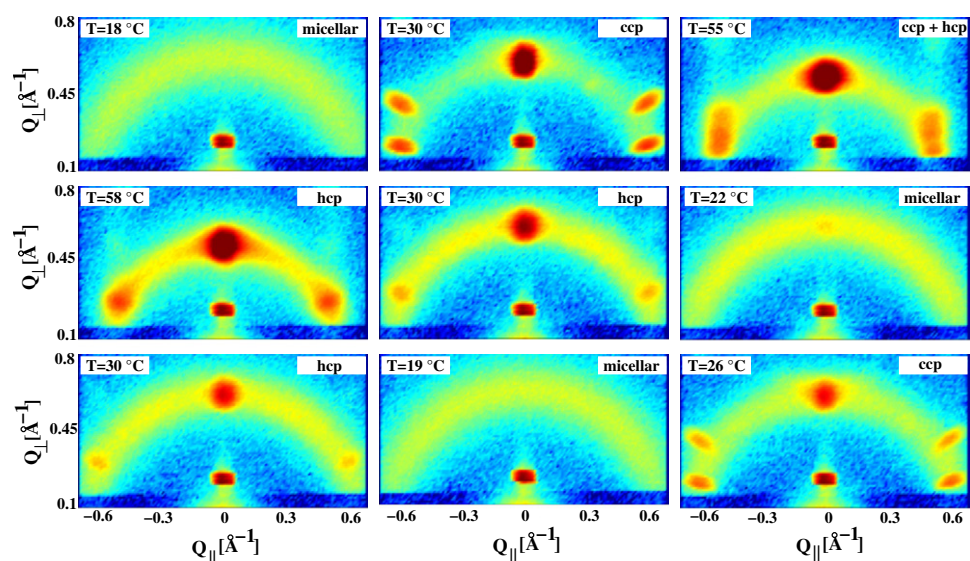
(3). The correlations quickly disappear with temperature for the repulsive one (correlations smaller than  $1 \mu\text{m}$  are beyond the accessible angular range).

Figure 3 shows the results of the GISANS measurements with the sample in contact with the attractive interface. At a temperature of  $17^\circ\text{C}$  the ring of increased intensity shows that the sample is in the micellar phase (1), while at  $30^\circ\text{C}$  the reflections reveal the presence of a cubic phase (2). At  $55^\circ\text{C}$  we find a coexistence of the cubic and the hexagonal phase before the hexagonal phase (4) is fully developed at  $58^\circ\text{C}$ . Surprisingly, while cooling the sample down to  $30^\circ\text{C}$ , the cubic phase does not reappear. But the hexagonal phase is still prevalent with increased diffuse scattering. With further cooling we reach the micellar phase at  $22^\circ\text{C}$ , however, with a weak reflection visible in the scattering plane. On heating the sample again to  $30^\circ\text{C}$  we regain the hexagonal phase. Only after cooling down to  $19^\circ\text{C}$  and completely melting the crystalline structure, the cubic phase is formed when the sample is heated.

Figure 4 shows the results for the sample in contact with the repulsive interface. At a temperature of  $17^\circ\text{C}$  we again find the micellar phase and at  $24^\circ\text{C}$  the cubic phase. In contrast to the attractive interface, for the repulsive one already at  $32^\circ\text{C}$  a coexistence between the cubic and the hexagonal phase shows up. The hexagonal phase is completely developed at  $58^\circ\text{C}$ . For  $80^\circ\text{C}$ , the crystalline structure is molten. While cooling the sample down from  $80$  to  $19^\circ\text{C}$  the hexagonal phase is always present, whereas the crystal melts at high and low temperatures.

#### 4. Conclusion

The data reveal that the cubic phase is only formed when the sample is heated from a unpercolated state with missing nucleation centres of a hexagonal structure. In the presence of nucleation centres the hexagonal structure always develops, but with an increased number of defects and crystallites of about the same size as for the cubic structure. When crossing the crystallization border from the rod-like micelle phase the hexagonal structure is always formed



**Figure 3.** GISANS pattern measured during a heating–cooling cycle (left to right) with the sample in contact with the attractive interface.

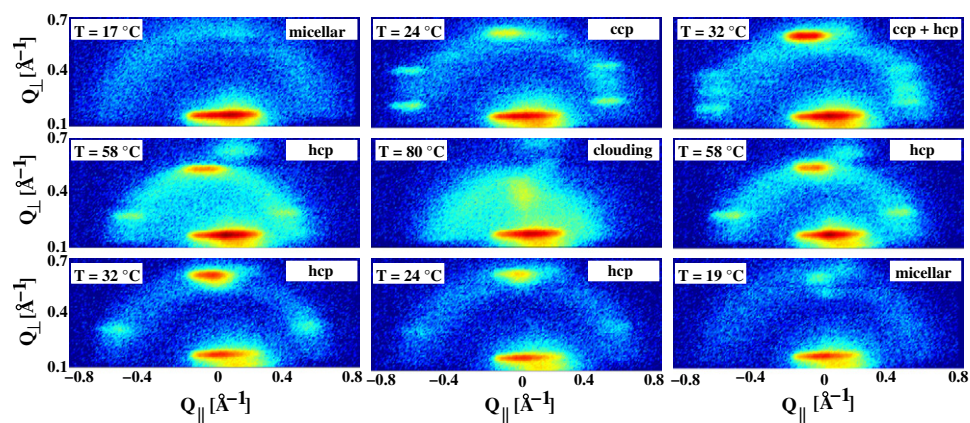


**Figure 4.** GISANS pattern measured during a heating–cooling cycle (left to right) with the sample in contact with the repulsive interface.

as the anisotropic particles prefer arranging in this lattice with lower symmetry as compared to the cubic one. The rod-like micelles show an increased preference to the repulsive interface, and without changing the crystalline structure long-range orientational correlations show up as the constraints of the crystal disappear and the rod-like micelles can orient parallel to the interface in the liquid phase (3). When crystallizing the cubic structure starting from low temperatures, first a very large correlation length or crystallite size develops, showing that the crystallization starts at several nucleation centres which grow rapidly. The sample is in a two-phase state with crystalline nuclei and micellar liquid. The scattering patterns reflect the interference of neutrons from a large sample volume (100  $\mu\text{m}$  in depth over an area of 8  $\text{cm}^2$  on the interface). As the crystalline phase is slightly denser the crystal may grow from

bottom to top. Relating to the long-range orientational correlations that develop parallel to the interface it is more likely that the micelles pre-crystallize close to the solid interface as expected for a colloidal system. Then the different crystallites start to interpenetrate and disturb each other. This results in a decreased correlation length seen as broadening of the rocking curve. For the attractive interface an equilibrium is then reached and the different crystallites rearrange, resulting in a decrease of the line width. For the repulsive interface the hexagonal structure immediately starts to develop, which results in a line width which is beyond the accessible  $q$ -range of our measurements. For the attractive interface the narrow component in the crystalline phases is more pronounced, demonstrating a preferred layering of micelles, whereas it is absent for the repulsive one, showing a suppressed crystallisation.

We have investigated the temperature dependence of the crystallization of the micellar polymer system P85 in deuterated water at interfaces with different surface–micelle interactions. We have found differences in the structures formed and in the correlation length at the different interfaces. In addition, while cooling the sample we always find the hexagonal structure close to both interfaces.

### Acknowledgments

This work has been supported by the BMBF (ADAM 03ZA6BC1). We acknowledge the help of B Deme during the measurement on D22.

### References

- [1] Ludwigs S *et al* 2003 *Nat. Mater.* **2** 744
- [2] Register R A 2003 *Nature* **424** 378
- [3] Cheng J Y *et al* 2002 *Appl. Phys. Lett.* **81** 3657
- [4] Noolandi J, Shi A-C and Linse P 1996 *Macromolecules* **29** 5907
- [5] Mallamace F *et al* 2000 *Phys. Rev. Lett.* **84** 5431
- [6] Chen W-R, Chen S-H and Mallamace F 2002 *Phys. Rev. E* **66** 021403
- [7] Khandpur A K *et al* 1995 *Macromolecules* **28** 8796
- [8] Berret J F *et al* 1994 *Europhys. Lett.* **25** 521
- [9] Linse P 1993 *Macromolecules* **26** 4437
- [10] Alexandridis P, Holzwarth J F and Hatton T A 1994 *Macromolecules* **27** 2414
- [11] Wanka G, Hoffmann H and Ulbricht W 1994 *Macromolecules* **27** 4145
- [12] Wolff M *et al* 2004 *Phys. Rev. Lett.* **92** 255501
- [13] Wolff M, Magerl A and Zabel H 2005 *Eur. Phys. J. E* **16** 141
- [14] Wolff M, Magerl A and Zabel H 2005 *Physica B* **357** 84
- [15] Mortensen K 2001 *Polym. Adv. Technol.* **12** 2
- [16] Carr W W *et al* 2001 *National Textile Center Annual Report*
- [17] Mortensen K 1996 *J. Phys.: Condens. Matter* **8** A103